EAI Endorsed Transactions
on Energy Web
Research Article EAI.EU

Variable Step-Size ANN-Based MPPT Controller for Standalone PV Systems under Varying Climatic Conditions

L. Salah[1,*], B. Ahmed[1], N. Ammar[1], K. Seyfallah[1], R. Abdelkrim[1], S. Nordine[1], Z. Abderrezzaq[1]
D. Rachid[1], S. Abdeldjalil[1], D. Abdeldjalil[1]

[1]Unité de Recherche en Energie Renouvelables en Milieu Saharien, URERMS, Centre de Développement des Energies Renouvelables, CDER, 01000 Adrar, Algeria

Abstract

The large-scale consumption of oil worldwide, combined with concerns about depletion, prompts investment in renewable energy sources to meet rising demand and mitigate the environmental impacts of fossil fuels. There are many renewable energy technologies, among which solar photovoltaic systems are particularly prominent. However, solar photovoltaic systems have some drawbacks due to intermittent irradiance, which generates volatile power output requiring cutting-edge technologies for effective utilization. In addition, conventional maximum power point tracking techniques often suffer from slow response and power oscillation that reduce energy yield. In this regard, an attempt is made to propose a technique that mitigates the aforementioned drawbacks in PV systems. For Maximum Power Point Tracking (MPPT), a Variable Step Size Artificial Neural Network Control (VSS-ANN) is used on solar PV systems in different scenarios and two meteorological experimental cases. The system is standalone, and the operating conditions are online. A comparative study has been made between the presented approach and other methods, such as Sliding Mode Control (SMC) and Perturb and Observe (P&O). The VSS-ANN approach ensures an advanced control framework to obtain the desired operation of the photovoltaic system in terms of limited fluctuations and stable operation by efficiently handling the maximum power point in a short time.

Keywords: PV system, MPPT, VSS-ANN, SMC, P&O

Received on 01 June 2025, accepted on 13 March 2026, published on 01 June 2026

doi: 10.4108/ew.9457

1. Introduction

The extent of the negative impact of conventional energy on the environment and its causing of global warming, added to the depletion of oil reservoirs, has prompted the active forces in the world to promote clean renewable energy sources and contribute effectively to energy generation in varying proportions between one country and another, relying on technological progress[1], [2]. Among these renewable energy sources, photovoltaic energy is at the forefront in terms of attention due to its abundance and environmental friendliness [3], [4], [5]. Photovoltaic farms usually convert solar radiation into electricity, and there are appropriate devices that make them usable as needed. Consequently, there are two types of photovoltaic systems: the first type is connected to the grid to help increase electrical power generation, and the second type is used in remote areas far from the main grid [6], [7], [8]. In Algeria, for example, grid-connected photovoltaic farms are used to support the national electricity grid. In contrast, stand-alone photovoltaic farms are used in the far south, where there are population centers, palm plantations, and other areas that are hundreds of kilometers away from the national grid (Fig.1) [9]. Photovoltaic systems have two main disadvantages, which are the inability to produce

*Corresponding author. Email: lachtarsalahba@gmail.com

maximum power under variable weather conditions, as well as the inefficiency of the system in bad weather or at night. Many studies have been conducted in this field to improve the performance of these systems and overcome the mentioned drawbacks. The ability of solar panels and their performance curve is affected by changing temperature and radiation, as changing radiation leads to a linear, direct change in current and a small direct change in voltage. While an increase in temperature leads to a decrease in the voltage and power produced and a slight increase in the current, which leads to the necessity of establishing a mechanism to track the MPPT and maintain it under conditions of continuously changing temperature and radiation [10]. In this regard, many countries have adopted projects in this field, which has prompted many specialized laboratories around the world to conduct research work to develop these photovoltaic systems and improve their performance. In addition to the development of solar modules, control units have also been developed that ensure high flexibility in tracking MPPT by analyzing the data provided by the installed sensors, using classical and then advanced control methods, and now, artificial intelligence techniques have been introduced [11]. The popular classical techniques are the short-circuit current and the open-circuit voltage methods, which require parameters to operate the photovoltaic system in various climatic conditions [12]. However, the drawback of these techniques is the lack of flexibility in tracking when the solar radiation and temperature are constantly changing, which makes them inaccurate. Advanced methods include more complex approaches to ensure flexible tracking, such as P&O, incremental conductance (INC), and SMC. However, these control techniques have drawbacks such as high oscillations and poor performance in volatile weather conditions [13].

As for artificial intelligence techniques, they include methods such as ANN, fuzzy logic (FL), particle swarm optimization (PSO), and advanced algorithms that ensure great flexibility and very high efficiency in MPPT tracking, regardless of how unstable or suddenly fluctuating the weather conditions are, and even under partial shade conditions. However, these methods suffer from two main drawbacks: they are expensive and very complex [14].

Direct methods generally rely on a fixed step size. The major drawback of these methods is their long response time in the case of a small step size, while the reaction in the case of a large step size is fast, but the tracking accuracy around the MPP is lost, which leads to energy loss [15]. To provide more flexible solutions to overcome this problem, an MPPT controller is introduced with a step size that varies depending on the photovoltaic panel's characteristics and weather fluctuations, thereby improving the tracking accuracy [16].

This work introduces a method for handling the MPPT tracking point to avoid these problems. An ANN-MPPT controller incorporates an additional factor to make it operate with a variable step size according to the environmental conditions necessary to control an autonomous solar plant. In this regard, the proposed method's effectiveness and reliability are verified through simulation in a Simulink/MATLAB environment by comparing it with other known methods. In addition, experimental results are presented.

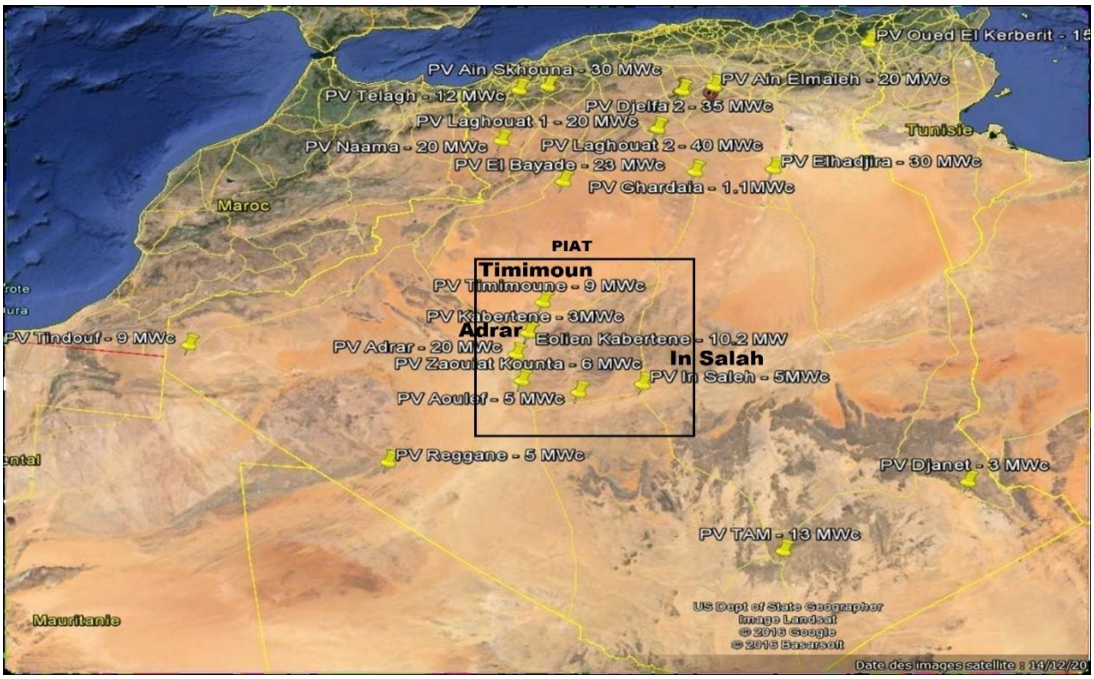

Figure 1. PV system distribution map in Algeria until 2018 [22]

2. Solar PV system

This scope uses a detailed solar energy system model, including different solar irradiance values and temperature impacts, compared to the equivalent PV system circuit, known as the single-diode model. More details on this structure PV system can be found in [17].

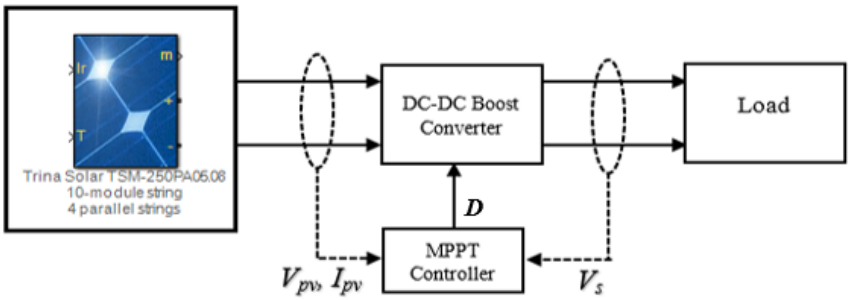

Figure 2. Solar PV system structure

Establish the following equation to determine the MPPT efficiency:

$$\eta_{MPPT} = \frac{\int_{t_1}^{t_2} P_{pv} dt}{\int_{t_1}^{t_2} P_{pv\_\max} dt} \quad (1)$$

t_1: The start-up time

t_2 : The shut-down time

P_{pv}: The PV power output

Photovoltaic energy is the direct conversion of sunlight into electricity using materials that absorb light photons and generate electron charges.

The solar cell is designed using an inverse parallel current-generating source Iph for the diode D. In addition, a parallel resistance Rsh and a series resistance Rs are added as a model to simulate the cell [3], [18], [19].

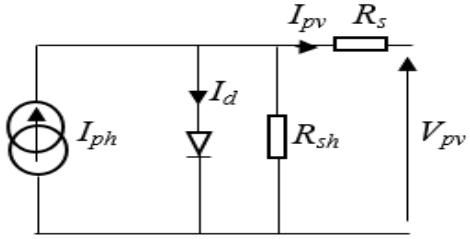

Figure 3. PV cell equivalent circuit

The terminal current of a solar cell can be expressed as:

$$I_{pv} = I_{ph} - I_d - I_{sh} \quad (2)$$

Where:

I_{pv} : output current of the PV cell (A).

I_{ph} : photogenerated current (A).

I_d : diode current (A).

I_{sh} : shunt current (A).

R_s : series resistance of the cell (Ω).

R_{sh} : parallel resistance of the cell (Ω).

The PV array output current is given as follows:

$$I_0 = I_{rs}[T/T_r]^3 exp\left[\left((qE_{g0}/aK) - \left(\frac{1}{T_r} - 1/T\right)\right)\right] \quad (3)$$

Where:

I_0 : reverse saturation current (A).

I_{rs} : saturation current at reference temperature (A).

a : diode ideality factor (1 for an ideal diode).

q : electron charge.

K : Boltzmann's constant.

T : absolute temperature (K).

T_r : reference temperature (K).

The PV system used in this paper to simulate the model in MATLAB/Simulink, as shown in Fig. 2, is a Trina Solar 250 W model with standard assumptions: the solar irradiance and temperature are 1000 W/m² and 25 °C, respectively. The studied system characteristics are 10 KW and 40 PV modules, 10 module strings, and 4 parallel strings.

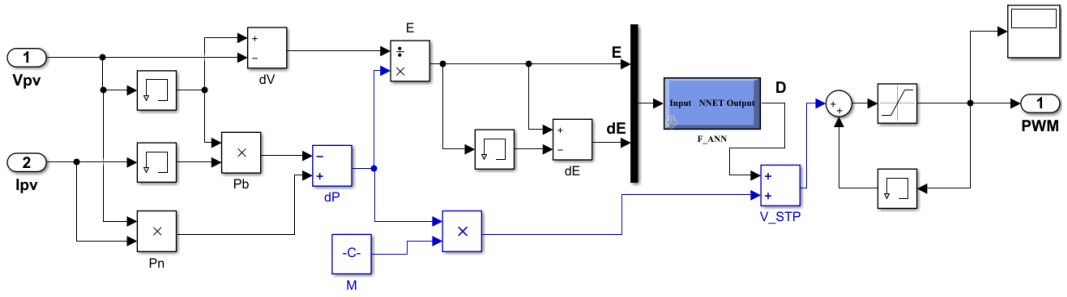

Figure 4. A VSS-ANN controller Simulink model

The main specifications of the PV module are shown in Table 1.

Table 1. PV array specification

Parameters	Value
PV module per string	10
Parallel connected strings	4
Cells per module (Ncell)	60
Open circuit voltage Voc (V)	37.6
Short circuit current Isc (A)	8.55
Voltage at MPP Vmp (V)	31
Current at MPP Imp(A)	8.06
Maximum power per module (w)	249.86

2.1 DC-DC boost converter modeling

A boost converter is used to raise the DC input voltage to a higher output voltage (Fig. 5). This boost converter includes a switch (S), an inductance (L), a diode that shields S as it prevents return current, and the capacitor C2 filtering the output voltage.

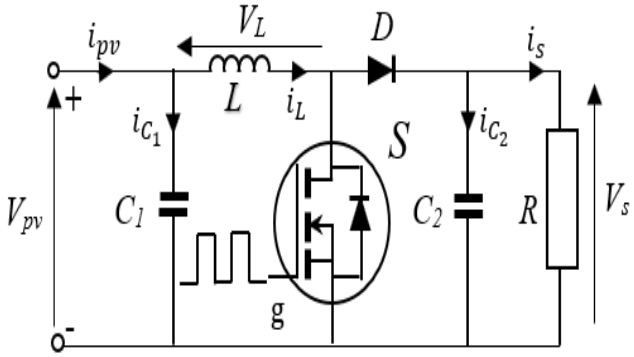

Figure 5. DC-DC boost converter

According to Fig. 5, it is easy to establish the following equation:

$$V_{pv}.D = \left(V_s - V_{pv}\right).\left(1-D\right) \tag{4}$$

The conversion report is written as follows:

$$V_s / V_{pv} \quad \text{Ĥ}\left(1-D\right) \quad D \in \quad \left[0 \quad 1\right] \tag{5}$$

3. VSS-ANN MPPT controller

The solar system is characterized by two-aim nonlinear curves presented by current/voltage and active power/voltage, which are influenced by temperature and radiation variations (Fig. 4).

Therefore, the MPP is influenced by climatic ambient conditions as it constantly adjusts its position in solar modules. Thus, solar models commonly use a DC-DC converter to transfer maximum power to the load using the variable step size duty ratio of pulse width modulation (PWM) in PV systems. Whereas the operation optimal point is tracked by the MPPT regulator. The variation from minimum to maximum step size between every perturbation or at the beginning of the day and its end are important factor in the MPPT controller's proper design. The duty cycle for the VSS method proposed is given as follows:

$$D(k) = D(k-1) \pm (D(k) + M * dp) \tag{4}$$

$$dp = p(k+1) - p(k) \tag{5}$$

Where:

The duty cycle $D(k)$ is the fixed step between k and $k-1$.

M is the scaling factor to regulate the step size.

A DC-AC inverter is applied to regulate the active/reactive power to get an AC voltage. Fig. 2 shows the input-side MPPT regulator.

As mentioned earlier, the fixed step size in conventional MPPT methods, despite its good performance, lacks flexibility in tracking when facing weather fluctuations, as fast tracking with a large step size with excessive oscillations is inevitable, while a small step size reduces these excessive oscillations but causes slow tracking [20].

This study proposes a flexible MPPT algorithm to deal with operational cases with the ability to change the step size to avoid the problems of excessive oscillations and slow tracking. Thus, it achieves better performance compared to conventional methods. Figure 4 shows the VSS-ANN-MPPT controller developed using Simulink:

In solar energy systems, the photovoltaic generator output power derivative (dP) and voltage derivative (dV) are generally used for monitoring. These two quantities are the

inputs to the artificial neural network, corresponding to solar radiation and cell operating temperatures that are subject to weather conditions.
The artificial neural network's output variable is the normalized duty cycle (±1).

Before training the ANN, a rigorous data preprocessing phase was conducted to ensure the quality and reliability of the input data. This preprocessing included [21]:

- Data normalization: Feature values were uniformly scaled to improve model convergence and performance.
- Missing Data Handling: Incomplete data were handled through imputation or exclusion, reducing potential bias.
- Feature Selection: The most relevant parameters were identified and retained to optimize model accuracy while avoiding overfitting.
- Dataset Distribution: The dataset was divided into subsets for training, validation, and testing to reliably assess the generalization capabilities of the model.

Effective data preprocessing is crucial for enhancing the accuracy and robustness of machine learning models, ensuring that predictions are reliable and generalize to new data.
After preprocessing, the ANN training process was launched using the Levenberg-Marquardt (LM) algorithm. The developed ANN architecture includes two input nodes and two hidden layers (each containing ten neurons), and one output node.
After running the algorithm under ideal conditions (25 °C and 1000 W/g), conditions_reversion, and according to different scenarios for 5 seconds, a dataset was created and collected from simulations based on MATLAB software. The data needed for training, validation, and testing were determined. 75% of the data was collected for training, 15% for validation, and 10% for testing. Figure. Figure 7 illustrates the ANN response.
The training results, as shown in Figures 6 and 7, confirm the successful convergence of the model, demonstrating its ability to accurately predict system behavior.

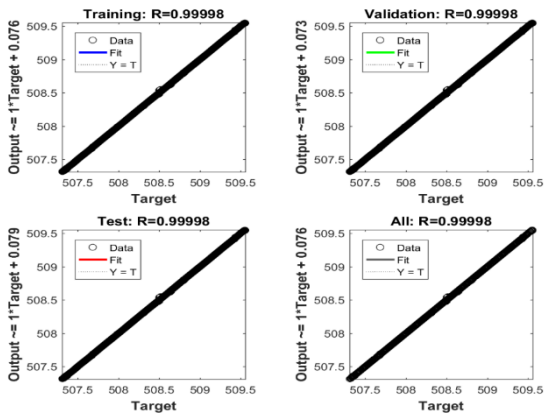

Figure 6. Training a regression neural network

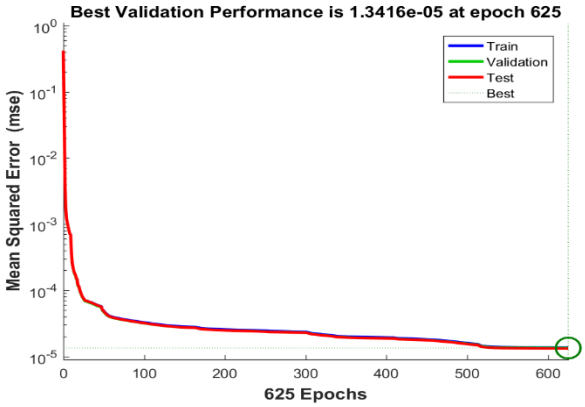

Figure 7. Training performance Neural network

4. Theoretical tests

Theoretical tests were conducted in the MATLAB/Simulink environment to compare the MMPT based on VSS-ANN with other MPPTs, such as P&O and SMC, using a constant step size. This includes tests with varying irradiance at a standard temperature of 25 °C.

4.1 Irradiance effect

The ANN control scheme was observed to reduce ripple and enhance response time. Compared to other conventional control schemes, it performs well under abrupt climatic conditions changes (Fig.8 (Zoom_1) and (Zoom_2)).
The algorithm sensitivity was assessed, and the developed control system performance was discussed, operating in a standalone mode. The irradiance value was changed every 0.8s and increased progressively in intervals [0s... 3.2s] and [4s, 5s], and decreased in the interval [3.2s, 4s] as shown in Fig. 8(a). Note that the temperature is fixed at 25 °C.
As can be seen, the ANN control scheme yielded satisfactory performance associated with small variations near the MPP and improved convergence speed compared to P&O and SMC methods.
In the event of a sudden change in weather conditions, the operating point fluctuations are limited, proving the proposed framework's desired performance. For different irradiance values, the output PV power is less than 10 kW except when the irradiance value is at 1 k w/m2, in which case, the output PV power is closer to 10 kW, as shown in Fig. 8(b).

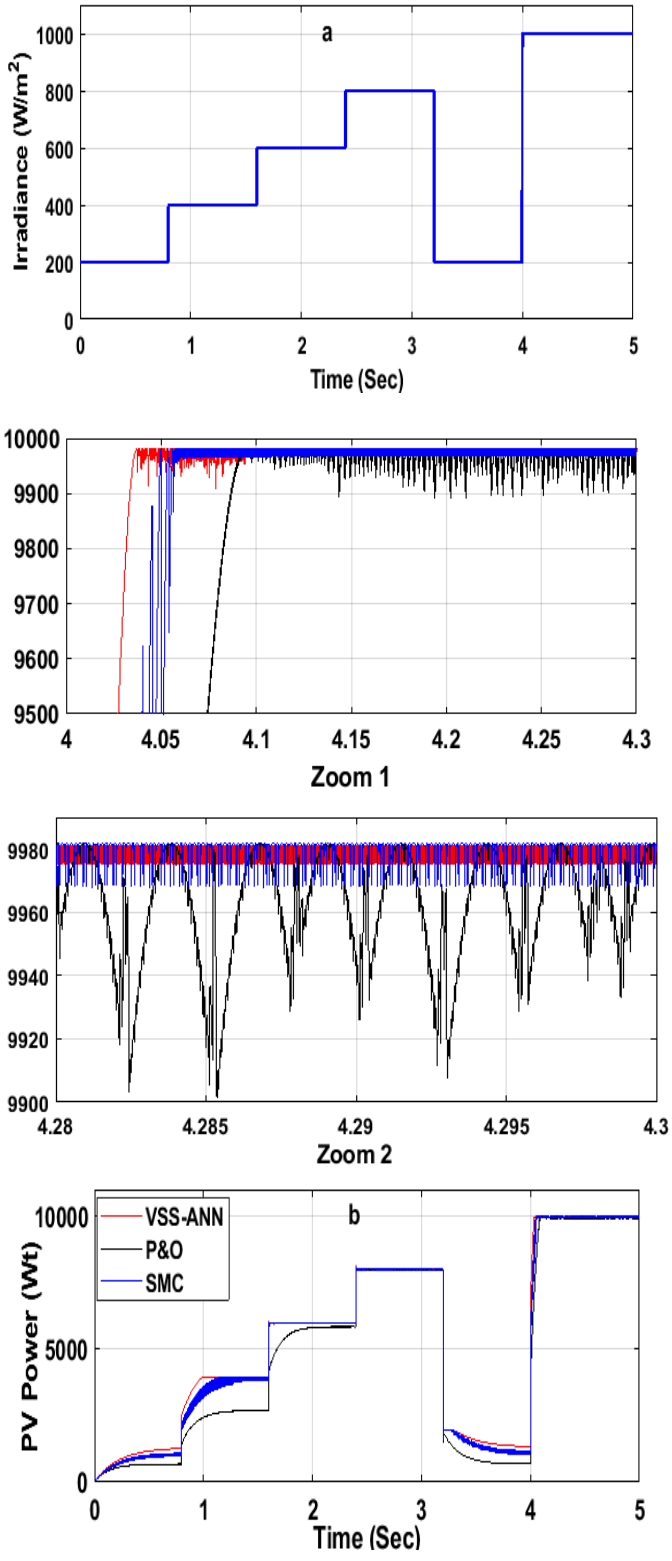

Figure 8. (a) Irradiance variation; (b) PV system output power

4.2 Temperature effect

This section evaluates the effect of temperature variations on the PV power output system, at a fixed standard irradiance value of 1000w/m2.

Fig. 9(a) illustrates the interval temperature variations, Fig. 9(b) shows the PV system output power generated under these temperature conditions, which demonstrates the satisfactory VS_ANN performance in terms of response speed and limited fluctuations compared to other methods, Fig. 9(b), (Zoom_1 and Zoom_2).

As mentioned earlier, the standard temperature of 25 °C yields an ideal PV system output power. However, when the temperature rises at t =2 Sec, Fig. 9(a), causes a decrease in PV system output power, where the initial decrease represents a transitional stage that causes some fluctuations around the MPP. Additionally, at temperatures higher than the standard temperature, there is a deficit in power generation from the PV power system, where the generated power is less than 10 Kw, Fig. 9(b).

Fig. 9(b) (Zoom_1 and Zoom_2) shows the obtained results in transient mode and steady-state mode under different methods with respect to temperature variations, where the VS_ANN demonstrates better performance in both transient and steady-state modes, compared to others.

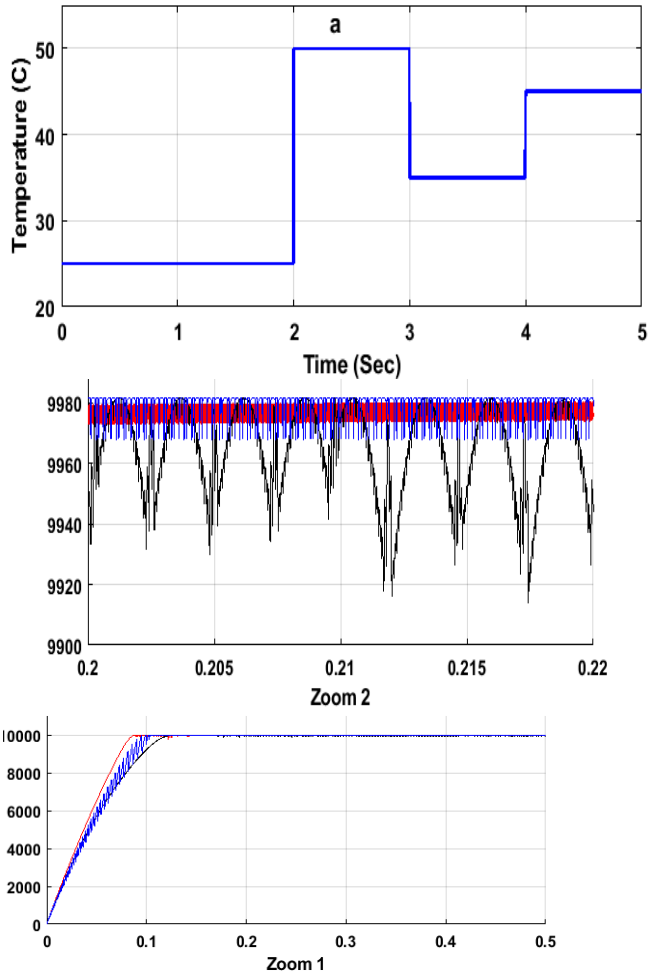

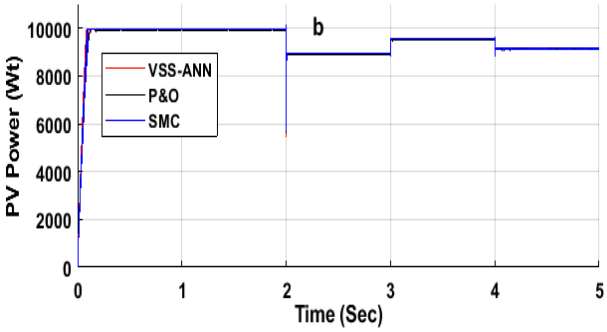

Figure 9. (a) Temperature variation, (b) PV system output power

5. Experimental test

In this applied work, we tried to verify the validity of the simulation results, as solar radiation and temperature data for February 17, 2023, were taken from the database located in the Renewable Energy Research Unit in the Desert Environment in Adrar, southern Algeria, and fed into the aforementioned system.

These data were fed into the same algorithm used in the previous simulations in the MATLAB environment, where they were compiled with a VSS-ANN, P&O, and SMC. Consequently, Figure. 10(a) shows the solar radiation captured by the pyranometer model CM 11, as shown in Figure. 11(a) for February 17, 2023, while the thermocouple type K is shown in Figure. 11(b) captured the temperatures for the same day as shown in Figure 10(b). The solar panel and its characteristics are shown in Figure 11 (c), and the EKO instruments MP 160 acquisition is shown in Figure 11 (d).

Figure 10(c) shows the MPP tracking using a conventional fixed step size P&O MPPT controller, a VSS-ANN-MPPT controller, and the SMC MPPT controller with a variable step hysteresis band surface that widens (divergence) in the transient state and narrows (convergence) in the steady state. According to Figure 10, Zoom1 and Zoom 2, the ANN and SMC have a speed-time response compared to P&O, with big fluctuations in SMC response due to the wider surface. In contrast, the ANN-MPPT exhibits small fluctuations and better efficiency compared to the other two controllers. Moreover, reduced ripple leads to less power waste, so the proposed ANN-MPPT controller demonstrated good performance in both experimental and simulation results.

According to the statistics data given in Fig.10 (c) presented in Table 2, VSS_ANN is faster at start-up time (start day) as it equals $-4.566*10^{-6}$ Wt compared to P&O and SMC, which are respectively -0.3467 Wt and -0.5373 Wt. The maximum Ppv power reaches the nominal Ppv power of the system, which is equal to 9645 Wt in steady state at midday for the VSS_ANN method. While in the other cases, P&O and SMC methods, Ppv is respectively 9622 Wt and 9632 Wt, which are the maximum powers at the same time mentioned above.

Table 2. Statistical data display on figure 10(c)

	X(sec)	Y (Wt)		
		VSS_ANN	P&O	SMC
Min	0	$-4.566*10^{-6}$	-0.3467	-0.5373
Max	5	9645	9622	9631
Mean	2.5	3905	3846	3786
Median	2.5	3272	2728	2849
Mode	0	$-4.566*10^{-6}$	-0.3467	-0.5373
std	1.443	3902	3880	3819
range	5	9645	9622	9632

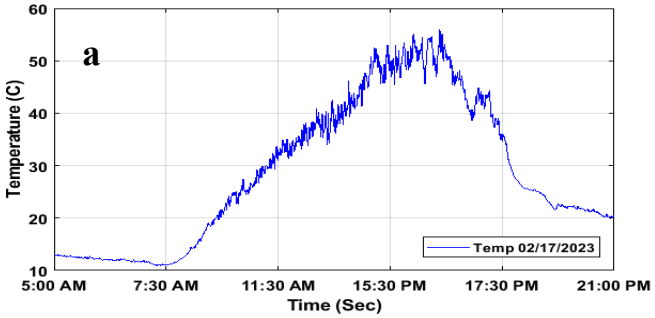

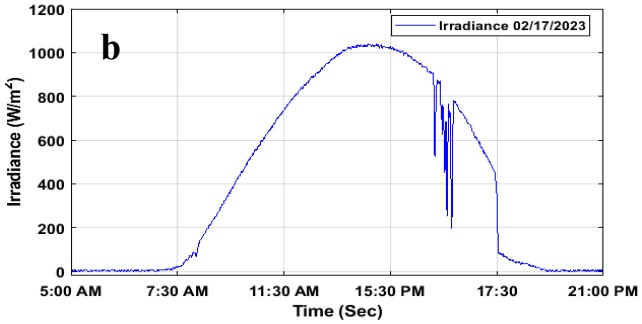

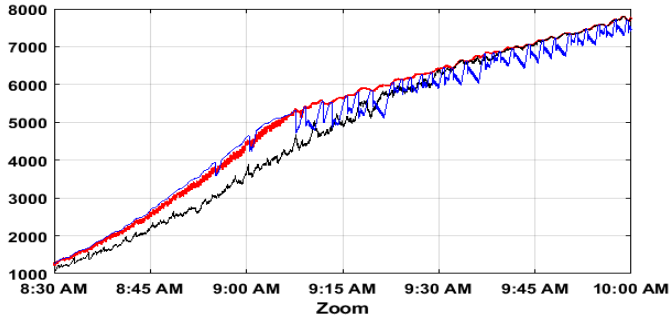

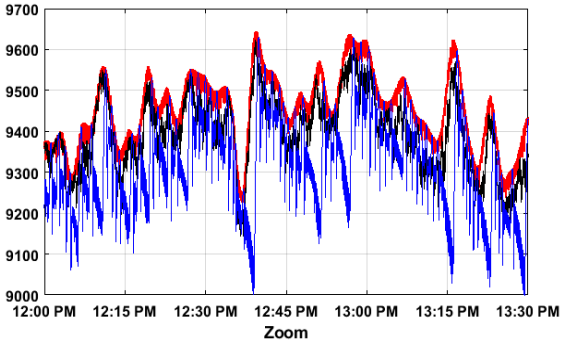

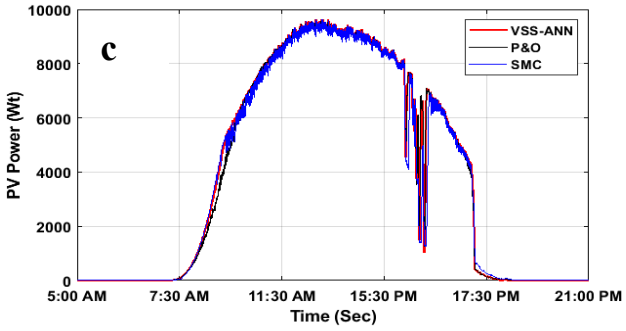

Figure 10. (a) Irradiance, (b) Temperature, (c) PV system output power

The collection of these experimental data was done by the devices represented in Figure 11 below.

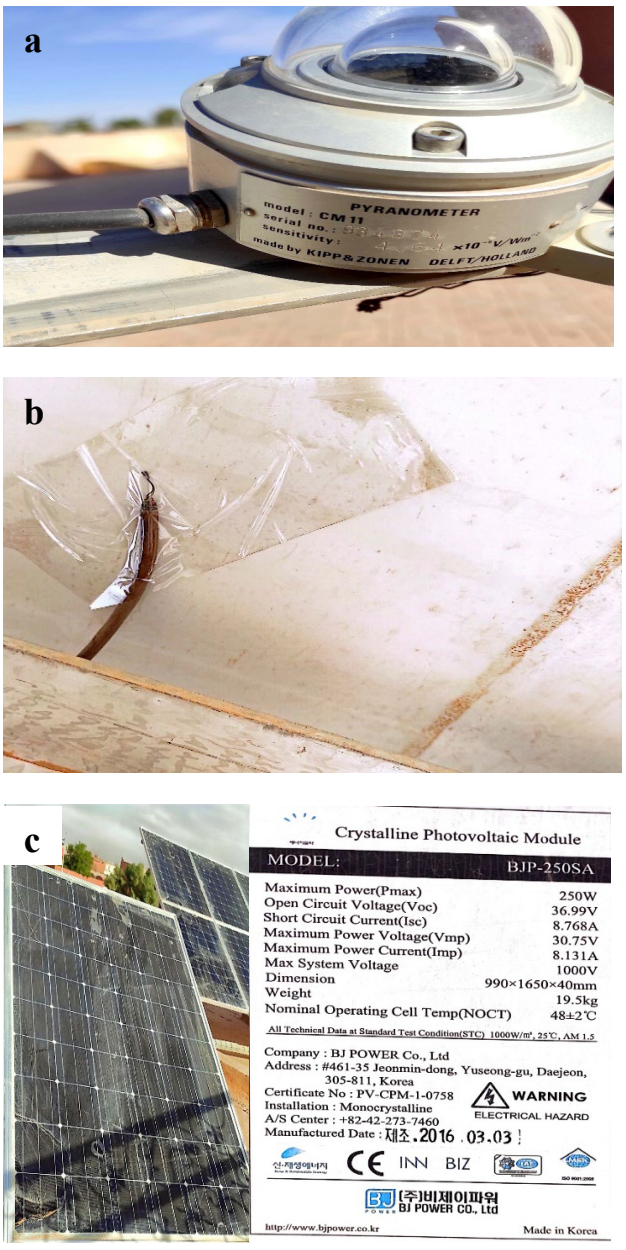

Figure 11. (a) Pyranometer CM11, (b) Thermocouple type K, (c) Solar panel BJP-250SA & its characteristics, (d) EKO instruments MP 160

6. Conclusion

In this paper, an ANN-MPPT controller has been proposed, operating in variable step size mode. Two other P&O and SMC conventional MPPTs are used, respectively, with fixed and variable step sizes according to the hysteresis band.

Both the simulation environment and experimental data results for the three proposed tracking methods are used and discussed in the simulation to demonstrate their performance and reliability.

The experimental data results used in the MATLAB environment showed that the VSS-ANN-MPPT controller responded quickly to changing weather conditions and was very flexible in tracking thanks to the variable step size, which helps reduce fluctuations in both the transient and steady states compared to both the P&O with a fixed step size and the SMC control with a hysteresis bond, which exhibits big oscillations in the transient state.

According to our analysis of the obtained results, the experimental results confirm the simulations, which show that the VSS-ANN-MPPT controller outperforms controllers with fixed step size or those using a hysteresis bond in both improving convergence through the response speed in the transient state and reducing oscillations size in both the transient and steady states, thereby reducing energy loss.

References

[1] A. Chabani, S. Makhloufi, and S. Lachtar, "Overview and impact of the renewable energy plants connected to the electrical network in southwest Algeria," *EAI Endorsed Transactions on Energy Web*, vol. 8, no. 36, pp. 1–15, 2021, doi: 10.4108/eai.29-3-2021.169168.

[2] D. Jeong, S. Hwang, J. Kim, H. Yu, and E. Park, "Public perspective on renewable and other energy resources: Evidence from social media big data and sentiment analysis," *Energy Strategy Reviews*, vol.

50, no. September, 2023, doi: 10.1016/j.esr.2023.101243.

[3] N. Yildiran and E. Tacer, "Identification of photovoltaic cell single diode discrete model parameters based on datasheet valuesYildiran, N., & Tacer, E. (2016). Identification of photovoltaic cell single diode discrete model parameters based on datasheet values. Solar Energy, 127, ," *Solar Energy*, vol. 127, pp. 175–183, 2016.

[4] M. A. A. Abdalla, W. Min, W. Bing, A. M. Ishag, and B. Saleh, "Double-layer home energy management strategy for increasing PV self-consumption and cost reduction through appliances scheduling, EV, and storage," *Energy Reports*, vol. 10, no. September, pp. 3494–3518, 2023, doi: 10.1016/j.egyr.2023.10.019.

[5] M. Benzaouia, A. Rabhi, B. Hajji, S. Benzaouia, H. Midavaine, and B. K. Oubbati, "Real-Time Control and Power Management Strategies of PV/Battery Standalone System," *IFAC-PapersOnLine*, vol. 56, no. 2, pp. 9135–9140, 2023, doi: 10.1016/j.ifacol.2023.10.151.

[6] S. Khattak, M. Yousif, S. U. Hassan, M. Hassan, and T. A. H. Alghamdi, "Techno-economic and environmental analysis of renewable energy integration in irrigation systems: A comparative study of standalone and grid-connected PV/diesel generator systems in Khyber Pakhtunkhwa," *Heliyon*, vol. 10, no. 10, p. e31025, 2024, doi: 10.1016/j.heliyon.2024.e31025.

[7] C. Dondariya *et al.*, "Performance simulation of grid-connected rooftop solar PV system for small households: A case study of Ujjain, India," *Energy Reports*, vol. 4, pp. 546–553, 2018, doi: 10.1016/j.egyr.2018.08.002.

[8] H. Belmili, S. Boulouma, B. Boualem, and A. M. Fayçal, "Optimized Control and Sizing of Standalone PV-wind Energy Conversion System," *Energy Procedia*, vol. 107, no. September 2016, pp. 76–84, 2017, doi: 10.1016/j.egypro.2016.12.134.

[9] "https://www.energy.gov.dz/Media/galerie/benational_2018-edition-2019_5dac85774bce1.pdf".

[10] Sameera, M. Tariq, and M. Rihan, "Analysis of the impact of irradiance, temperature and tilt angle on the performance of grid-connected solar power plant," *Measurement: Energy*, vol. 2, no. May, p. 100007, 2024, doi: 10.1016/j.meaene.2024.100007.

[11] P. Li, J. Zhang, R. Xu, J. Zhou, and Z. Gao, "Integration of MPPT algorithms with spacecraft applications: Review, classification and future development outlook," *Energy*, vol. 308, no. May 2024, 2024, doi: 10.1016/j.energy.2024.132927.

[12] A. Nadeem, H. A. Sher, A. F. Murtaza, and N. Ahmed, "Online current-sensorless estimator for PV open circuit voltage and short circuit current," *Solar Energy*, vol. 213, no. November 2020, pp. 198–210, 2021, doi: 10.1016/j.solener.2020.11.004.

[13] R. G. Mohamed, H. M. Hasanien, and M. A. Ebrahim, "Global MPPT controllers for enhancing dynamic performance of photovoltaic systems under partial shading condition," *e-Prime - Advances in Electrical Engineering, Electronics and Energy*, vol. 9, no. June, p. 100638, 2024, doi: 10.1016/j.prime.2024.100638.

[14] S. Gul, S. M. Malik, Y. Sun, and F. Alsaif, "An Artificial Neural Network Based MPPT Control of Modified Flyback Converter for PV Systems in Active Buildings," *Energy Reports*, vol. 12, no. August, pp. 2865–2872, 2024, doi: 10.1016/j.egyr.2024.08.082.

[15] E. Korany, D. Yousri, H. A. Attia, A. F. Zobaa, and D. Allam, "A novel optimized dynamic fractional-order MPPT controller using hunter pray optimizer for alleviating the tracking oscillation with changing environmental conditions," *Energy Reports*, vol. 10, pp. 1819–1832, 2023, doi: 10.1016/j.egyr.2023.08.038.

[16] A. Loukriz, M. Haddadi, and S. Messalti, "Simulation and experimental design of a new advanced variable step size Incremental Conductance MPPT algorithm for PV systems," *ISA Trans.*, vol. 62, pp. 30–38, 2016, doi: 10.1016/j.isatra.2015.08.006.

[17] L. Salah, B. Wafa, N. Ammar, B. Ahmed, and Z. Abderrezzaq, "Improvement of the Dismc Method Via Ismc To Provide a Faster Response Time and Mitigate Chattering Phenomenon," *UPB Scientific Bulletin, Series C: Electrical Engineering and Computer Science*, vol. 84, no. 1, pp. 189–200, 2022.

[18] H. H. Ammar, A. T. Azar, R. Shalaby, and M. I. Mahmoud, "Metaheuristic Optimization of Fractional Order Incremental Conductance (FO-INC) Maximum Power Point Tracking (MPPT)," vol. 2019, 2019.

[19] S. N.B. and S. D, "A novel Beluga Whale Optimization for maximum power tracking in photovoltaic systems under shading and non-shading conditions," *Energy Reports*, vol. 12, pp. 4352–4373, Dec. 2024, doi: 10.1016/j.egyr.2024.10.010.

[20] S. Messalti, A. Harrag, and A. Loukriz, "A new variable step size neural networks MPPT controller: Review, simulation and hardware implementation," *Renewable and Sustainable Energy Reviews*, vol. 68, no. August 2015, pp. 221–233, 2017, doi: 10.1016/j.rser.2016.09.131.

[21] S. J. SeyedShenava, P. Zare, and I. F. Davoudkhani, "Maximizing solar energy harvesting efficiency: Optimal hybrid deep neural learning - based MPPT for Photovoltaic systems under complex partial shading conditions," *Sustainable Computing: Informatics and Systems*, vol. 47, Sep. 2025, doi:

10.1016/j.suscom.2025.101159.
conditions_reversion
[22] A. Chabani, S. Makhloufi, and S. Lachtar, “Overview and impact of the renewable energy plants connected to the electrical network in southwest Algeria,” *EAI Endorsed Transactions on Energy Web*, vol. 8, no. 36, pp. 1–15, 2021, doi: 10.4108/eai.29-3-2021.169168.